

conformations of these molecules in solution.

Acknowledgment. A grant from the National Science Foundation supported this work. The ^{19}F spectra were obtained with thanks to Dr. Armitage, Lewis Kay, and Carla Forte of Yale University. All other high-field spectra used were obtained at the Northeast Regional NSF-NMR Facility at Yale University.

We thank Dr. Hägele for supplying the ultrapure phosphonic and phosphinic acids.

Registry No. H, 1333-74-0; ^7Li , 13982-05-3; ^{11}B , 14798-13-1; ^{17}O , 13968-48-4; ^{35}Cl , 13981-72-1; ^{37}Cl , 13981-73-2; ^{39}K , 14092-91-2; ^{79}Br , 14336-94-8; ^{81}Br , 14380-59-7; N_2 , 7727-37-9; Na, 7440-23-5; I_2 , 7553-56-2.

Electrochemical Switching in Anthraquinone-Substituted Carbon-Pivot Lariat Ethers and Podands: Chain Length Effects in Geometric and Electronic Cooperativity[†]

Deborah A. Gustowski, Milagros Delgado, Vincent J. Gatto, Luis Echegoyen,* and George W. Gokel*

Contribution from the Department of Chemistry, University of Miami, Coral Gables, Florida 33124. Received June 12, 1986

Abstract: A series of 1-substituted anthraquinones has been synthesized, most often by nucleophilic aromatic substitution on 1-chloroanthraquinone. They have the following structures and were prepared in the indicated yields where E is $-\text{CH}_2\text{CH}_2-$ and Ar is the 1-substituted anthraquinone: **1**, Ar-OCH₃ (48%); **2**, Ar-OEOEOCH₃ (61%); **3**, Ar-OEOEOEOCH₃ (61%); **4**, Ar-OEOEOEOEOCH₃ (65%); **5**, Ar-OEOEOEOEOEOCH₃ (14%); **6**, Ar-OEOEOEO-Ar (66%); **7**, Ar-O-CH₂-15-crown-5 (39%). Both one- and two-electron time-resolved redox couples (using cyclic voltammetry) are observed for the various systems when 0-1.0 equiv of Li^+ , Na^+ , or K^+ are added. The electrochemical behavior is complex and is accounted for by a combination of electronic and steric factors.

Molecular switching in macrocyclic polyether systems has been the subject of intense study during the past decade. Photochemical switching has been especially well-studied in Japan by Shinkai, Ueno, Takagi, Tabushi, and others.¹ In addition, changes in pH,² thermally-controlled permeability,³ and oxidation-reduction chemistry⁴ have all been explored as switching mechanisms. The work conducted in our group has been primarily concerned with electrochemical switching in lariat ethers and podands having nitroaromatic sidearms⁵ and more recently has been focussed on similar species derived from anthraquinones.⁶ Anthraquinones differ significantly from the nitroaromatic systems in their ability to undergo discrete one- or two-electron reduction. We have previously noted that anthraquinone-substituted podands exhibit surprising geometrical effects during the electrochemical switching process.⁷ We now report the details of the switching process and describe the geometrical and electronic cooperativity we have observed for the Li^+ , Na^+ , and K^+ -mediated electrochemical reductions in anthraquinone-substituted podands and lariat ethers.

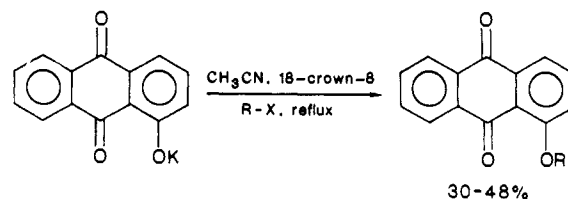
Results and Discussion

Syntheses. Three methods have been used to prepare the anthraquinone-substituted podands and lariat ethers. Method A (Scheme I) involves the reaction of the potassium salt of 1-hydroxyanthraquinone with the appropriate halide or tosylate in the presence of a solvent and 18-crown-6.

In the absence of 18-crown-6, the reaction does not give any of the desired product. This is not surprising since the potassium salt of 1-hydroxyanthraquinone, due to ion-pairing interactions, is a very poor nucleophile. Nakatsuji et al. report that reaction of the sodium salt of 1,8-dihydroxyanthraquinone with triethylene glycol ditosylate in refluxing xylene gives only 0.6% yield of the bis(anthraquinone) crown 8.⁸

In the presence of 18-crown-6, the potassium is stripped from the anthraquinone anion increasing its nucleophilicity and giving reasonable yields of desired product. The compounds prepared by using this reaction are listed in Table I as method A.

Scheme I

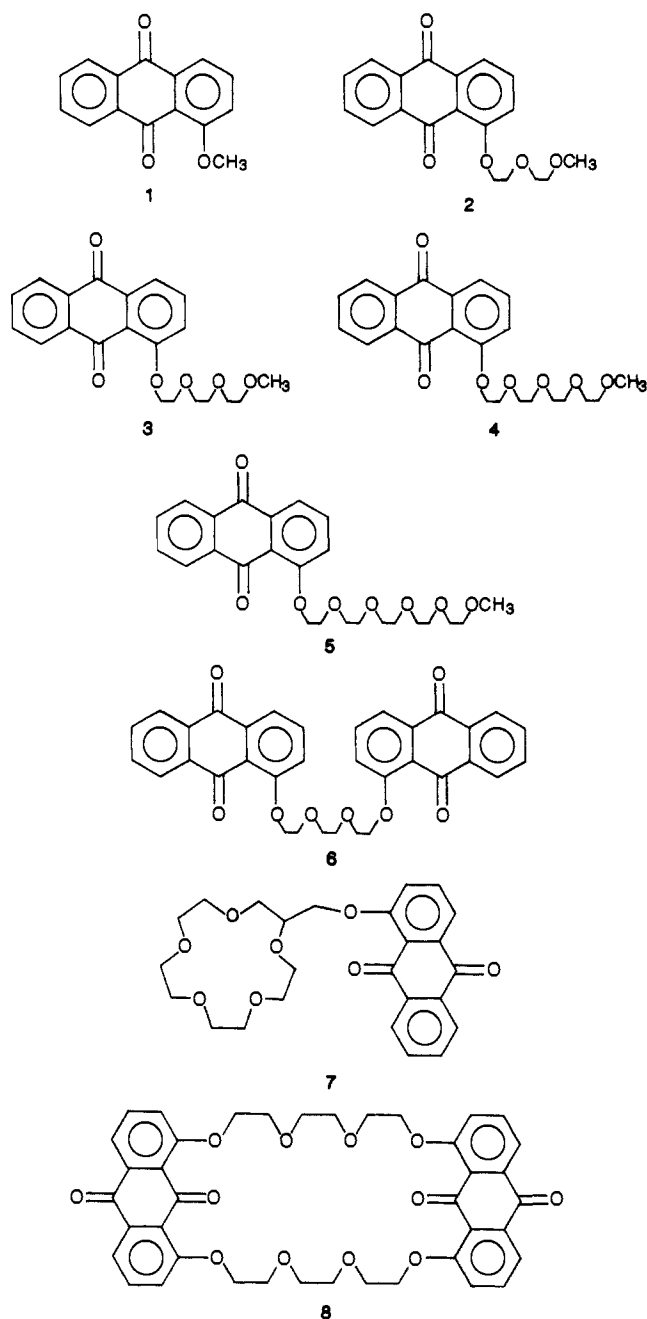


Method B (Scheme II) is a modification of the procedure reported by Krapcho and Shaw⁹ and is more straightforward than

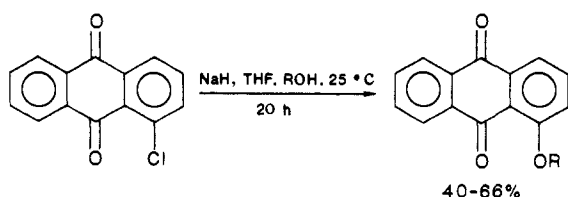
- (1) (a) Shinkai, S.; Shigematsu, K.; Kusano, Y.; Manabe, O. *J. Chem. Soc., Perkin Trans. 1* **1981**, 3279. (b) Shinkai, S.; Minami, T.; Kusano, Y.; Manabe, O. *Tetrahedron Lett* **1982**, 2581. (c) Nakamura, H.; Nishida, H.; Takagi, M.; Ueno, K. *Bunseki Kagaku* **1982**, *31*, E131. (d) Shinkai, S.; Ogawa, T.; Kusano, Y.; Manabe, O.; Kikukawa, K.; Goto, T.; Masuda, T. *J. Am. Chem. Soc.* **1982**, *104*, 1960. (e) Shinkai, S.; Minami, T.; Kusano, Y.; Manabe, O. *J. Am. Chem. Soc.* **1982**, *104*, 1967. (f) Shinkai, S.; Minami, T.; Kouno, T.; Kusano, Y.; Manabe, O. *Chem. Lett.* **1982**, 499.
- (2) (a) Takahashi, M.; Takamoto, S. *Bull. Chem. Soc. Jpn.* **1977**, *50*, 3414. (b) Stetter, H.; Frank, W. *Angew. Chem., Int. Ed. Engl.* **1976**, *15*, 686. (c) Desreux, J. F. *Inorg. Chem.* **1980**, *19*, 1319. (d) Stetter, H.; Frank, W.; Mertens, R. *Tetrahedron* **1981**, *37*, 767. (e) Tazaki, M.; Nita, K.; Takagi, M.; Ueno, K. *Chem. Lett.* **1982**, 571. (f) Nakamura, H.; Nishida, H.; Takagi, M.; Ueno, K. *Anal. Chim. Acta* **1982**, *139*, 219. (g) Charewicz, W. A.; Bartsch, R. A. *Anal. Chem.* **1982**, *54*, 2300. (h) Shinkai, S.; Kinda, H.; Araragi, Y.; Manabe, O. *Bull. Chem. Soc. Jpn.* **1983**, *56*, 559. (i) Tsukube, H. *Tetrahedron Lett.* **1983**, *24*, 1519. (j) Tsukube, H. *J. Chem. Soc., Perkin Trans. 1* **1983**, 29. (k) Izatt, R. M.; Lamb, J. D.; Hawkins, R. T.; Brown, P. R.; Izatt, S. R.; Christensen, J. J. *Am. Chem. Soc.* **1983**, *105*, 1782.
- (3) Shinkai, S.; Nakamura, S.; Tachiki, S.; Manabe, O.; Kajiyama, T. *J. Am. Chem. Soc.* **1985**, *107*, 3363.
- (4) (a) Shinkai, S.; Inuzuka, K.; Miyazaki, O.; Manabe, O. *J. Am. Chem. Soc.* **1985**, *107*, 3950. (b) Bock, H.; Hierholzer, B.; Vogtle, F.; Hollman, G. *Angew. Chem., Int. Ed. Engl.* **1984**, *23*, 57. (c) Wolf, R. E.; Cooper, S. R. *J. Am. Chem. Soc.* **1984**, *106*, 4646.
- (5) (a) Kaifer, A.; Echegoyen, L.; Gustowski, A.; Goli, D.; Gokel, G. W. *J. Am. Chem. Soc.* **1983**, *105*, 7168. (b) Gustowski, D.; Echegoyen, L.; Goli, D. M.; Kaifer, A.; Schultz, R. A.; Gokel, G. W. *J. Am. Chem. Soc.* **1984**, *106*, 1633. (c) Morgan, C. R.; Gustowski, D. A.; Cleary, T. P.; Echegoyen, L.; Gokel, G. W. *J. Org. Chem.* **1984**, *49*, 5008. (d) Kaifer, A.; Gustowski, D. A.; Echegoyen, L.; Gatto, V. J.; Schultz, R. A.; Cleary, T. P.; Morgan, C. R.; Goli, D. M.; Rios, A. M.; Gokel, G. W. *J. Am. Chem. Soc.* **1985**, *107*, 1958.

[†] For the previous parts in this series, see ref 5.

Chart I



Scheme II



method A for a variety of reasons.

First, one less step is involved because the alcohol does not need to be converted into the halide or tosylate. Second, the reaction may be conducted at room temperature and gives purer product

(6) Echegoyen, L.; Gustowski, D. A.; Gatto, V. J.; Gokel, G. W. *J. Chem. Soc., Chem. Commun.* **1986**, 220-223.

(7) Gustowski, D. A.; Delgado, M.; Gatto, V. J.; Echegoyen, L.; Gokel, G. W. *Tetrahedron Lett.* **1986**, 3487-3490.

(8) Nakatsuji, S.; Ohmori, Y.; Iyoda, M.; Nakashima, K.; Akiyama, S. *Bull. Chem. Soc. Jpn.* **1983**, 3185.

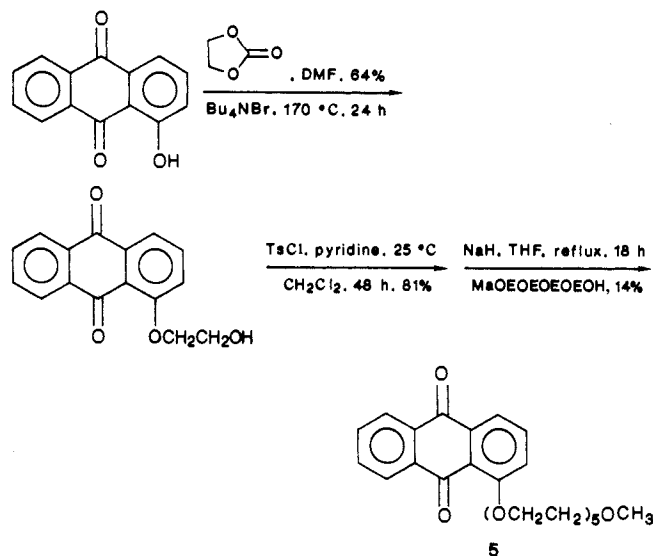
(9) Krapcho, A. P.; Shaw, K. J. *J. Org. Chem.* **1983**, *48*, 3341.

Table I. Syntheses of Anthraquinone-Substituted Podands and Lariat Ethers

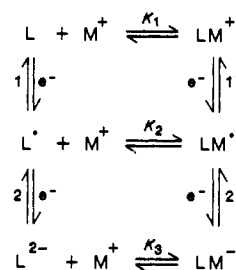
compd	method	starting alcohol ^a	yield (%)	mp (°C)
1	A ^b	1-hydroxyanthraquinone	48	170-171
2	B	MeOEOEOH	61	62-64
3	B	MeOEOEOEOH ^c	61	55-57
4	B	MeOEOEOEOEOH	65	70-72
5	C	MeOEOEOEOEOH	14	48-49
6	A	1-hydroxyanthraquinone	30	170-173
	B	HOEOEOEOH	66	
7	A	1-hydroxyanthraquinone	39	100-102
	B	15-crown-5-CH ₂ -OH	40	

^a See experimental section for details; E represents the -CH₂CH₂- unit. ^b See text for a description of methods. ^c Alcohol (2 equiv) used.

Scheme III



Scheme IV



mixtures than does method A. Of course, the greater reactivity of alkoxides compared to the 1-anthroxides is not surprising and allows these reactions to be conducted in the absence of 18-crown-6. Third, and related to the latter, the reaction is rapid: it is usually complete in 1-2 h. The compounds prepared by using this reaction are listed in Table I as method B.

Preparation of the anthraquinone podand 5 was attempted by using the method illustrated in Scheme III. This approach (listed in the table as method C) gave very poor yields of the anthraquinone-substituted podand. The lack of success with this method is the result of two factors. First, the tosylate is very insoluble in most organic solvents even at elevated temperatures. Second, elevated temperatures lead to *p*-toluenesulfonic acid elimination in the presence of base.

Electrochemistry. All electrochemical results were obtained in MeCN containing tetra-*n*-butylammonium perchlorate (0.1 M) by using a glassy carbon working electrode, and ligands were present at 10⁻³ M concentration. Scan rates between 100 and 200 mV/s were used. The results obtained are recorded in Table II and summarized in Scheme IV.

Some general observations concerning the data obtained are as follows. The work of Fujinaga et al. on simple quinone systems

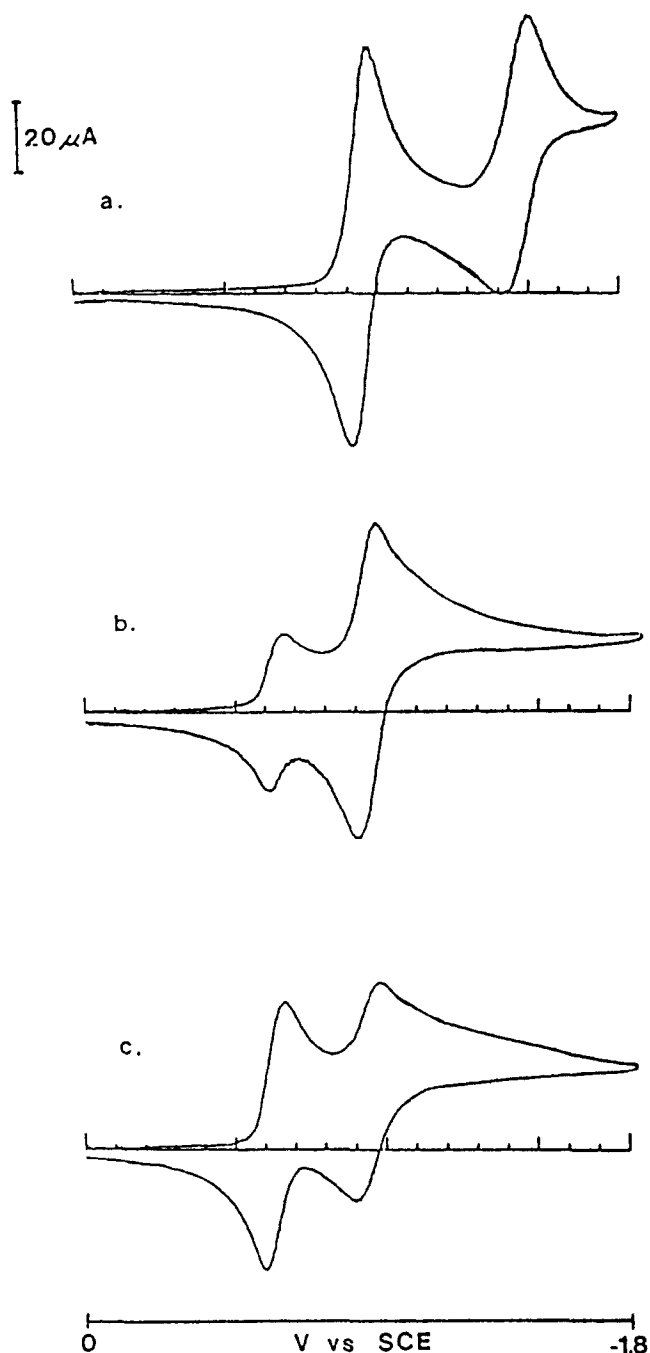


Figure 1. Cyclic voltammograms for **2** (a) in the absence of Li^+ , (b) in the presence of 0.5 equiv of Li^+ , and (c) in the presence of 1.0 equiv of Li^+ .

shows the usual time-averaged shifts in redox potentials as a function of metal ion concentrations.¹⁰ Our unique systems show time-resolved redox pairs upon addition of alkali metal salts. These couples correspond to steps 1, 1', 2, and 2' in Scheme IV. The presence of lithium cation results in the observation of a new redox couple corresponding to step 1' in Scheme IV (see Figure 1). It is interesting to note that for none of the systems studied is a new redox wave observed which corresponds to step 2' in Scheme IV. This contrasts with the results obtained for sodium cation where two new time-resolved redox couples corresponding to steps 1' and 2' are observed in most cases (see Figure 2). The situation in the presence of potassium cation is exactly the reverse of that for lithium, i.e., only the new redox couple corresponding to step 2' is observed and that for step 1' is absent.

(10) (a) Nagaska, T.; Okazaki, S.; Fujinaga, T. *J. Electroanal. Chem.* **1982**, *133*, 89. (b) Nagaoka, T.; Okazaki, S.; Fujinaga, T. *Bull. Chem. Soc. Jpn.* **1982**, *55*, 1967.

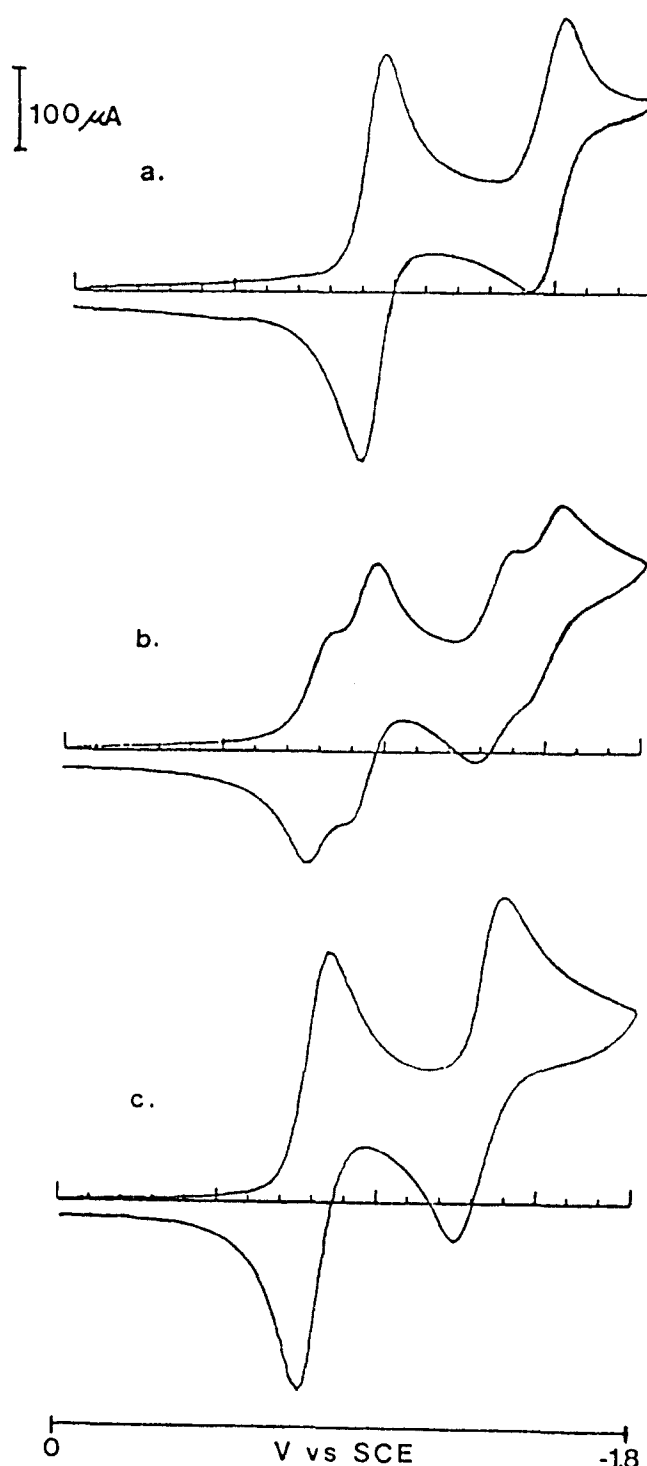


Figure 2. Cyclic voltammograms for **4** (a) in the absence of Na^+ , (b) in the presence of 0.5 equiv of Na^+ , and (c) in the presence of 1.0 equiv of Na^+ .

As the podand chain length increases, we note the following trends for each cation (refer to Table III). For lithium, the potential difference between steps 1' and 1 increases from **1** to **2** and then remains constant for **3**, **4**, and **5**. When sodium cation is present, a similar trend is observed, with leveling occurring after **2**. A striking contrast is found for the difference in potential between steps 2' and 2 for both sodium and potassium. For these, potential differences decrease monotonically as the number of side-arm oxygen atoms increases. For all of the cations studied, lariat ether **7** behaves differently for reasons discussed below.

Ligands and Lithium Cation. As anticipated from a consideration of Coulombic effects and as observed in previous studies of electrochemically switched systems, the largest electrochemically

Table II. Cation Dependence of Quinone Electrochemistry

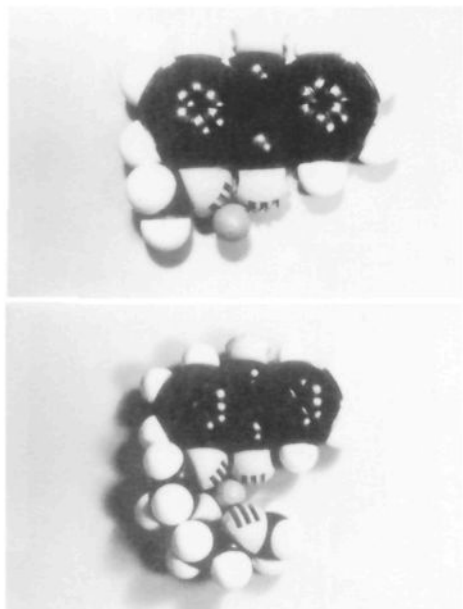
compd no.	cation	E_p^{c1}	E_p^{a1}	E^{o1}	E_p^{c2}	E_p^{a2}	E^{o2}	E_p^{c3}	E_p^{a3}	E^{o3}	E_p^{c4}	E_p^{a4}	E^{o4}	ΔE^{1-2}	enhancement ^a (K_3/K_2)	ΔE^{3-4}	enhancement (K_2/K_1)	
1	none	-1.48	-1.41	-1.44				-0.90	-0.85	-0.88								
	Li ⁺	0.5	-1.47	-1.38	-1.42	-1.18 ^b		-0.91	-0.84	-0.88	-0.68	-0.62	-0.65			0.23	7.7×10^3	
		1.0	-1.46	-1.37	-1.42	-1.18		-0.92	-0.83	-0.88	-0.69	-0.60	-0.64					
	Na ⁺ c	0.5	-1.46	-1.39	-1.42	-1.30	-1.20	-1.25	-0.91	-0.86	-0.88				0.17	7.5×10^2		
		1.0	-1.45	-1.39	-1.42	-1.28	-1.18	-1.23	-0.91	-0.86	-0.88							
2	none	-1.47	-1.38	-1.42				-0.94	-0.86	-0.90								
	Li ⁺	0.5	-1.46	-1.35	-1.40			-0.94	-0.86	-0.90	-0.62	-0.58	-0.60			0.30	1.2×10^5	
		1.0	-1.40	-1.35	-1.38	-1.23	-1.13	-1.18	-0.92	-0.82	-0.87	-0.87	-0.76	-0.82	0.20	2.4×10^3	0.05	7
	Na ⁺	0.5	-1.47	-1.39	-1.43	-1.34	-1.26	-1.30	-0.92	-0.84	-0.88				0.13	1.6×10^2		
		1.0	-1.45	-1.41	-1.43	-1.34	-1.24	-1.29	-0.91	-0.85	-0.88							
3	none	-1.49	-1.41	-1.45				-0.94	-0.88	-0.91								
	Li ⁺	0.5	-1.44	-1.32	-1.38			-0.94	-0.88	-0.91	-0.64	-0.60	-0.62			0.29	8.0×10^4	
		1.0	-1.46	-1.32	-1.38			-0.93	-0.87	-0.90	-0.64	-0.58	-0.61					
	Na ⁺	0.5	-1.46	-1.41	-1.44	-1.34	-1.26	-1.30	-0.93	-0.89	-0.91	-0.81	-0.76	-0.78	0.14	2.3×10^2	0.13	1.6×10^2
		1.0	-1.45	-1.38	-1.42	-1.38	-1.28	-1.33	-0.94	-0.85	-0.90	-0.81	-0.73	-0.77	0.09	33		
4	none	-1.49	-1.39	-1.44				-0.93	-0.86	-0.90								
	Li ⁺	0.5						-0.93	-0.82	-0.88	-0.62	-0.54	-0.58			0.30	1.2×10^5	
		1.0						-0.93	-0.82	-0.88	-0.63	-0.52	-0.58					
	Na ⁺	0.5	-1.47	-1.39	-1.43	-1.32	-1.24	-1.28	-0.92	-0.86	-0.89	-0.79	-0.73	-0.76	0.15	3.4×10^2	0.13	1.6×10^2
		1.0	-1.47	-1.39	-1.43	-1.32	-1.19	-1.26	-0.92	-0.86	-0.89	-0.80	-0.72	-0.76				
5	none	-1.48	-1.41	-1.44				-0.91	-0.81	-0.86								
	Li ⁺	0.5	-1.39	-1.27	-1.33			-0.89	-0.78	-0.86								
		1.0	-1.48	-1.41	-1.44			-0.92	-0.86	-0.89								
	Na ⁺	0.5	-1.46	-1.39	-1.42	-1.33	-1.19	-1.26	-0.90	-0.82	-0.86	-0.75	-0.69	-0.72	0.16	5.1×10^2	0.14	2.3×10^2
		1.0	-1.46	-1.39	-1.42	-1.33	-1.18	-1.25	-0.90	-0.82	-0.86	-0.75	-0.70	-0.72				
6	none	-1.48	-1.41	-1.44				-0.90	-0.80	-0.85								
	Li ⁺	0.5	-1.47	-1.40	-1.44			-0.90	-0.81	-0.85								
		1.0	-1.46	-1.35	-1.40			-0.92	-0.87	-0.90								
	Na ⁺	0.5	-1.42	-1.29	-1.36			-0.92	-0.87	-0.90	-0.62	-0.58	-0.60			0.30	1.2×10^5	
		1.0	-1.40	-1.28	-1.34			-0.92	-0.82	-0.85	-0.61	-0.57	-0.59					
7	none	-1.44	-1.30	-1.37				-0.91	-0.86	-0.88								
	Li ⁺	0.5	-1.41	-1.31	-1.36			-0.90	-0.83	-0.86	-0.75	-0.70	-0.72			0.14	2.3×10^2	
		1.0	-1.40	-1.30	-1.35			-0.89	-0.82	-0.86	-0.74	-0.70	-0.72					
	Na ⁺	0.5	-1.40	-1.30	-1.35			-0.89	-0.82	-0.86	-0.74	-0.70	-0.72					
		1.0	-1.40	-1.32	-1.36			-0.90	-0.84	-0.87								
7	none	-1.44	-1.30	-1.37				-0.88	-0.80	-0.84								
	Li ⁺	0.5	-1.44	-1.30	-1.37			-0.91	-0.86	-0.88								
		1.0	-1.49	-1.29	-1.39			-0.91	-0.84	-0.88	-0.71	-0.65	-0.68			0.20	2.4×10^3	
	Na ⁺	0.5	-1.40	-1.30	-1.35			-0.91	-0.83	-0.87	-0.71	-0.62	-0.66					
		1.0	-1.39	-1.31	-1.35			-0.90	-0.83	-0.86	-0.74	-0.71	-0.72			0.14	2.3×10^2	
7	Li ⁺	0.5	-1.42	-1.29	-1.36			-0.90	-0.83	-0.86								
		1.0	-1.39	-1.29	-1.36			-0.87	-0.81	-0.84								

^aEnhancements are calculated when 0.5 equiv of cation is present. ^bAdsorption peak. ^cAdsorption only observed.

Table III. Summary of Electrochemically Induced Cation Binding Enhancements (Reported as ΔE 's (V)) in Podands^a

compd no.	monoanion			dianion		
	Li ⁺	Na ⁺	K ⁺	Li ⁺	Na ⁺	K ⁺
1	0.23	ads ^b	NO ^c	NO ^c	ads	0.17
2	0.30	0.05	NO ^c	NO ^c	0.20	0.13
3	0.29	0.13	NO ^c	NO ^c	0.14	0.09
4	0.30	0.13	NO ^c	NO ^c	0.15	NO ^c
5	0.30	0.14	NO ^c	NO ^c	0.16	NO ^c
6	0.30	0.14	NO ^c	NO ^c	NO ^c	NO ^c
7	0.20	0.14	NO ^c	NO ^c	NO ^c	NO ^c

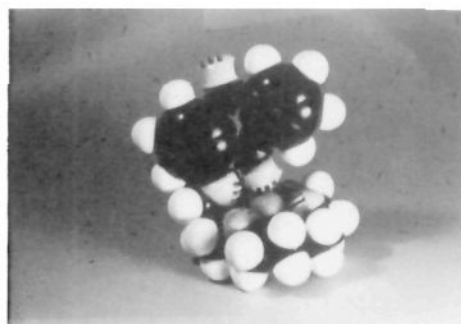
^a Enhancements in V when 0.5 equiv of cation is present. For enhancement factors and other values, see Table II. ^b Adsorption. ^c NO means "not observed," i.e., no new redox couple was observed.

**Figure 3.** Corey-Pauling-Koltun (CPK) molecular models of **1** (top) and **2** (bottom) in the presence of Li⁺.

induced cation binding enhancements (K_2/K_1) are observed when lithium cation is present. The absence of an electrochemical couple corresponding to 2 and 2' in Scheme I is probably the result of rapid electron transfer between L^{•-} and LM[•]. Precedent for this behavior has been reported¹¹ for the case in which protons rather than metal cations were "complexed". This behavior is observed only for Li⁺ which is more like H⁺ than any of the other cations studied. Although the data do not unequivocally confirm this, it seems to be a likely explanation.

The 1-oxyanthraquinone ligand has an interesting structural feature not found in most of the other lariat ether and podand compounds prepared thus far. One of the carbonyl oxygens is in a peri relationship with the 1-oxygen. Upon reduction of the anthraquinone residue, the largest increase in spin density occurs on the >C=O oxygens. An examination of CPK molecular models (see Figure 3) shows that the small lithium cation fits nicely into the cavity between the carbonyl oxygen atom and the adjacent ether oxygen of **1**. Neither Na⁺ nor K⁺ is small enough to do so. When two additional oxygen atoms are present in the side chain (as in **2**), a tetrahedron of donor groups surrounds Li⁺. This appears to be the best arrangement for solvation of Li⁺. Such an optimal solvation arrangement results in the greatest electrochemical enhancement (K_2/K_1). The addition of more oxygen atoms in compounds **3**, **4**, and **5** is irrelevant because use of more remote side chain oxygens to solvate the cation reduces the direct effect of the carbonyl group. The cation binding enhancement thus levels off after a total of four oxygen atoms are present.

In bisanthraquinone podand **6**, four oxygen atoms are available to solvate a lithium cation associated with only one of the two aromatic residues. The cation binding enhancement should be

**Figure 4.** CPK molecular model of **7** in the presence of Na⁺.

near 0.30 as observed for the other podand systems and is found to be 0.30.

In the monopodand compounds, the polyether side chain is attached directly to the 1-oxygen of anthraquinone whereas a macrocyclic ring is attached to anthraquinone in **7**. From our examination of CPK molecular models, we conclude that the podands are more flexible than the lariat ether. The more flexible side chain can interact with the anthraquinone-bound cation more effectively than can the crown ring leading to a stronger ion pair between lithium cation and the anion radical. The stronger interaction leads to a greater binding enhancement in **1-6** than is observed for **7**.

Single-Electron Reduction in the Presence of Sodium Cation.

As expected for less charge-dense sodium cation, the electrochemically induced binding enhancements are smaller with this cation than those observed for lithium cation. We have previously noted that **1** in the presence of Na⁺ is adsorbed to the electrode surface preventing the observation of an electrochemical wave.⁷ An examination of CPK molecular models suggests that the same situation as described for Li⁺ applies to the sodium cation. As a result of different cation sizes, the leveling is observed after **3** rather than after **2**. The cation binding enhancement is also smaller as a result of the lower charge density for Na⁺ compared to Li⁺. The magnitude of this difference may also reflect the variation in binding geometries for Li⁺ compared to Na⁺. In the latter case, the donor group arrangement appears less favorable than the obviously optimal arrangement for Li⁺. In the sodium case, the binding geometry with lariat ether **7** appears optimal, as illustrated in Figure 4. Although the crown itself is less flexible than are the podands, the donor group arrangement is such that maximal, three-dimensional solvation is achieved.

Single-Electron Reduction in the Presence of Potassium Cation.

As noted above, the initial redox couple (1') is not observed for ligands in the presence of K⁺. In the case of K⁺, we cannot directly determine the ratio K_2/K_1 because no redox couple was observed for process 1'. This is because the neutral quinone has only a small affinity for K⁺ (i.e., K_1 is small). The concentration of LK⁺ (LM⁺ in Scheme II) is therefore small and little reduction occurs over pathway 1'.

Two-Electron Reduction in the Presence of Na⁺ and K⁺. We have already accounted for the absence of a Li⁺ cation effect on dianion formation in solution (see above). The effects of Na⁺ and K⁺ on reduction of the monoanion are similar to each other but differ from the Li⁺ case.

Lithium cation exerts a very strong influence on the neutral ligands because of its charge density and because of the special geometric arrangements described above. Sodium cation cannot assume such a favorable geometrical arrangement and is less charge dense, so single-electron transfer is perturbed less than for the Li⁺ case. When Na⁺ interacts with the anthraquinone monoanion, it exerts a strong influence due to ion pairing and thus strongly perturbs transfer of the second electron. As before, when the geometrical arrangement of donor groups is more favorable (compounds **3-5** compared to **2**), sodium cation's influence is diminished and leveled.

The effect of K⁺ on electron transfer can be explained in similar terms. The effect of K⁺ on dianion formation is larger than on

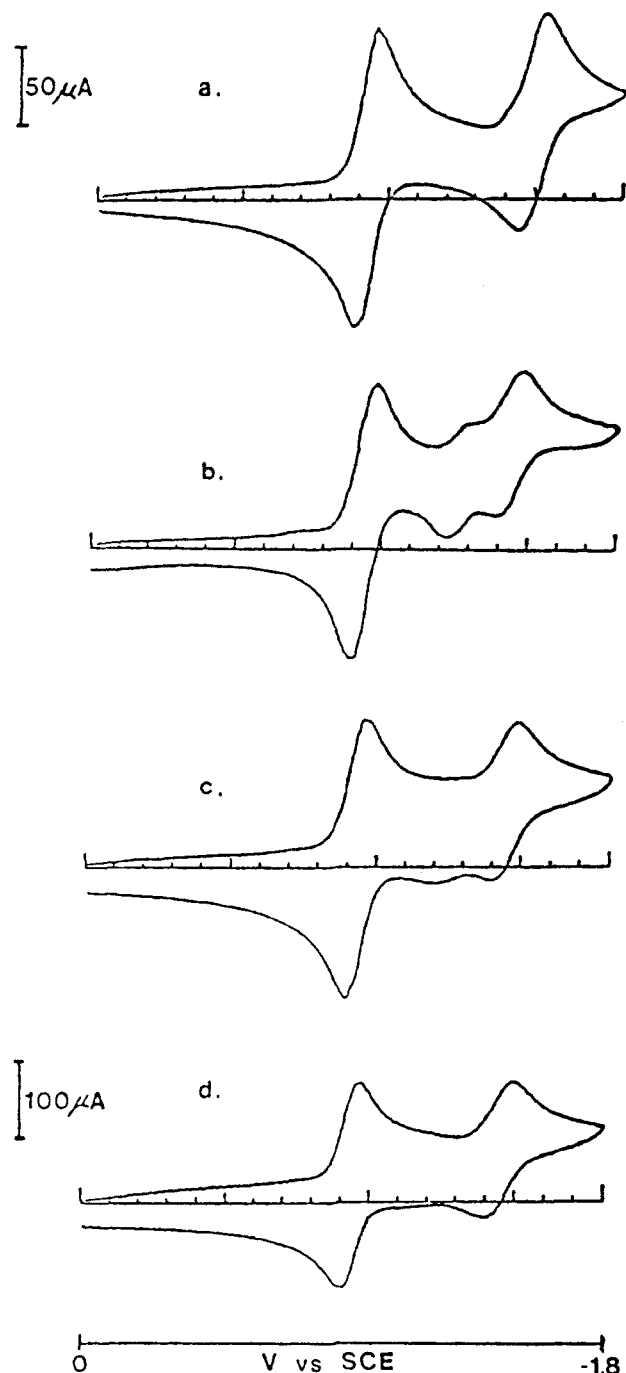


Figure 5. Cyclic voltammograms for **1** (a) alone and in the presence of 0.5 equiv of K^+ using scanning rates of (b) 100 mVs^{-1} , (c) 500 mVs^{-1} , and 1000 mVs^{-1} .

monoanion formation because of ion pairing in the dianion complex. Its effect is less than for sodium cation because of its lower charge density and because of the less favorable geometry required for complexation. As with Na^+ , however, the effect of K^+ also diminishes with increasing chain length.

The effect of K^+ on neutral ligands is small and even less than with Na^+ . As a consequence, no cation effect on monoanion formation is observed. One possible pathway of reduction is $L \rightarrow L^{\cdot-}$ via electrochemical step 1. If sufficiently slow, chemical step K_2 can then compete effectively with electrochemical step 2. This results in the observation of all three redox processes, 1, 2, and 2'. As a result, LK^- is obtained despite the absence of reaction along pathway 1'. This analysis is supported by a variable scan rate study. The cyclic voltammetry was conducted in the presence of 0.5 equiv K^+ at 100, 500, and 1000 mV/s , respectively (see Figure 5). At the lower scan rates, there is enough time between successive reductions (1, 2) so that equilibrium K_2

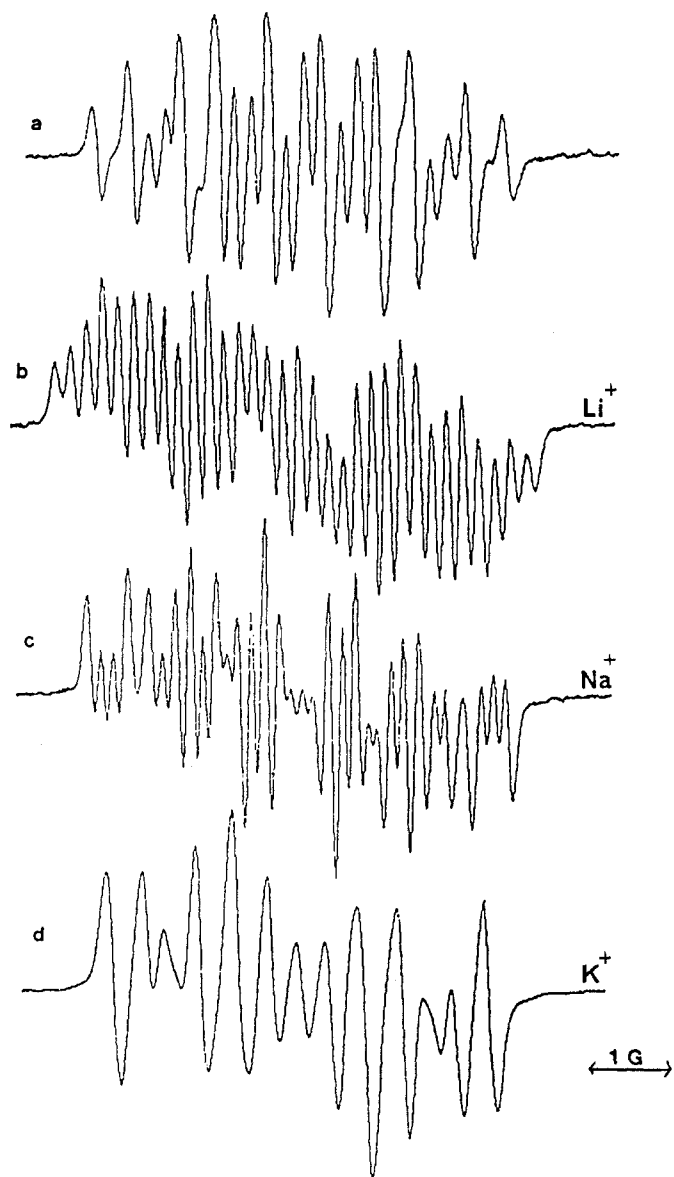


Figure 6. ESR spectra of **4** (10^{-4} M in THF) (a) in the absence of cations and in the presence of 1 equiv each of (b) Li^+ , (c) Na^+ , and (d) K^+ .

partially competes with pathway 2. Redox couple 2' is therefore clearly observed. As the scan rate increases, pathway 2 dominates until, at 1000 mV/s , redox couple 2' is totally inhibited. Other pathways may be possible.

Electron Spin Resonance Studies. The extent of interaction between the reduced anthraquinone portion of **4** and Li^+ , Na^+ , and K^+ was assessed by using ESR spectroscopy. The experimentally observed ESR spectra for free $4^{\cdot-}$ and for $4^{\cdot-}$ in the presence of each cation are shown in Figure 6. The experimentally determined spectra were simulated by using the following coupling constants (in G): for free $4^{\cdot-}$ $A_{2H} = 0.45$, $A_{1H} = 0.67$, $A_{2H} = 1.08$, $A_{1H} = 1.34\text{ G}$, $w = 0.11\text{ g}$ (Figure 6a); for $4^{\cdot-}\cdot Na^+$ $A_{1H} = 0.57$, $A_{1H} = 0.65$, $A_{1H} = 0.81$, $A_{1H} = 1.22$, $A_{1H} = 1.53$, $A_{Na^+} = 0.17$, $w = 0.11$ (Figure 6c); for $4^{\cdot-}\cdot K^+$ $A_{1H} = 0.43$, $A_{1H} = 0.67$, $A_{1H} = 0.84$, $A_{1H} = 1.11$, $A_{1H} = 1.58$, $w = 0.21\text{ G}$ (Figure 6d). No K^+ splitting was observed in the latter case. In the case of Li^+ , the spectral lines have not been fully assigned due to its complexity, but a Li^+ splitting of 0.22 G was apparent. These results confirm the strong intramolecular ion pairing interactions observed by using electrochemical techniques.

Summary

The syntheses of several novel anthraquinone-substituted polydands and an analogous lariat ether are described. The electrochemical behavior of these compounds has been studied in the

absence and presence of Li^+ , Na^+ , and K^+ . Distinct new time-resolved redox couples are observed in various cases in the range 0–1.0 equiv of cation for both one- and two-electron transfer processes. This contrasts the work of Fujinaga et al. where only shifts in E° 's are observed upon addition of alkali metal salts.¹⁰ As we have observed previously,⁵ cation binding is enhanced more when Li^+ cation is present than when other cations are added. This is attributed to a Coulombic effect. The complicated electrochemical behavior can be accounted for by considering both the electronic effects of the various donors and the geometrical arrangements possible with each compound.

Experimental Section

General Methods. ^1H NMR spectra were recorded on a Hitachi Perkin-Elmer R-600 high resolution NMR spectrometer in CDCl_3 solvent and are reported in ppm (δ) downfield from internal Me_4Si . IR spectra were recorded on a Perkin-Elmer 599 infrared spectrophotometer and were calibrated against the 1601-cm^{-1} band of polystyrene. Melting points were determined on a Laboratory Devices Mel-Temp and are uncorrected.

Thin-layer chromatographic analyses were performed on aluminum oxide 60 F-254 neutral (type E) or silica gel 60 F-254 having a 0.2-mm layer thickness. Preparative chromatography columns were packed with aluminum oxide, activated, neutral Brockmann 1 (150 mesh, standard grade), or with Kieselgel 60 (70–230 mesh). Chromatotron with 2-mm thick circular plates prepared from Kieselgel 60 PF-254.

Reagents for Syntheses. All reagents were the best grade commercially available and were used without further purification unless otherwise noted. Tetrahydrofuran (THF) was dried over Na° /benzophenone indicator prior to use. All commercial grade solvents (CHCl_3 , CH_2Cl_2 , hexanes, acetone) were distilled prior to use. Molecular distillation temperatures refer to the oven temperature of a Kugelrohr apparatus. Combustion analyses were performed by Atlantic Microlab, Inc., Atlanta, Ga.

Reagents for Electrochemistry. Acetonitrile (Alfa) was distilled from CaH_2 and P_2O_5 . Tetrahydrofuran (THF, Aldrich) was flask-to-flask distilled from Na/K in a vacuum line immediately prior to use. All solutions were prepared under an atmosphere of dry N_2 . Tetrabutylammonium perchlorate (TBAP, Fluka) was twice recrystallized from EtOAc and stored in a desiccator. Alkali-metal perchlorate salts were recrystallized from deionized water and dried in a vacuum oven at 100°C for 24 h.

Cyclic Voltammetry Experiments. The electrochemical experiments were performed at 25°C under N_2 in MeCN 0.1 M in TBAP. The electroactive species was present in millimolar concentrations. Glassy carbon was used as the working electrode and a Pt wire as the counter-electrode. E° values are reported vs. saturated calomel electrode (SCE). The measurements were done on a Bioanalytical Systems (Model 100) electrochemical analyzer, equipped with IR compensation, and recorded on a Houston DMP-40 plotter.

ESR Measurements. ESR spectra were recorded for dry THF solutions by using the X-band of an IBM ER-200D SRC spectrometer. Samples were prepared under vacuum (10^{-3} mm) by reaction of a 10^{-3} M solution of the compound with either lithium, sodium, or potassium metal as described in detail elsewhere.¹² The spectrum in the absence of metal was obtained by controlled-potential electrolysis by using TBAP as supporting electrolyte, directly in the ESR cavity. The potential was controlled between -0.9 and -1.1 V by using a Hewlett-Packard Model 6200B constant voltage supply.

Potassium Salt of 1-Hydroxyanthraquinone, KHA. 1-Hydroxyanthraquinone (11.2 g, 0.05 mol) and DMF (125 mL) were stirred in a 500-mL, round-bottomed flask while heating to dissolve the anthraquinone. Potassium *tert*-butoxide (6.2 g, 0.055 mol) was added to the reaction mixture in small portions (to control the exothermicity) during 30 min. The reaction mixture was allowed to cool during 1 h and transferred to a freezer. The resulting precipitate was filtered and dried under vacuum (75°C , 0.05 mm) for 3 h. The potassium salt of 1-hydroxyanthraquinone (a purple solid, 12.0 g, 92%) was used without further purification.

1-Methoxyanthracene-9,10-dione (1). KHA (above, 2.62 g, 0.01 mol), CH_3I (15 mL), and 18-crown-6 (2.64 g, 0.01 mol) were heated at reflux

temperature for 48 h. After having cooled the reaction mixture, CHCl_3 (50 mL) and HCl (50 mL, 3 N) were added. The phases were separated, the aqueous portion was extracted with CHCl_3 (25 mL), and the organic phases were washed with H_2O (25 mL) and brine (25 mL), dried (MgSO_4), and then concentrated in vacuo. Column chromatography (silica gel 60, CHCl_3 /hexanes, 2/3) followed by crystallization (EtOH) afforded **1** (1.15 g, 48%) as a yellow solid, mp $170\text{--}171^\circ\text{C}$ (lit.¹³ mp 169°C).

1-(2-(2-Methoxyethoxy)ethoxy)anthracene-9,10-dione (2). Diethylene glycol monomethyl ether (1.32 g, 11 mmol) was added to a suspension of NaH (60% oil dispersion, 0.64 g, 16 mmol) in dry THF (15 mL) under N_2 . After stirring for 20 min, 1-chloroanthraquinone (2.7 g, 11.1 mmol) was rinsed in by using dry THF (10 mL). The mixture was heated under reflux while stirring for 3 h, cooled, and concentrated in vacuo. The residue was added to H_2O (50 mL), extracted with CHCl_3 (2×50 mL), washed with brine (20 mL), dried (MgSO_4), and concentrated in vacuo. Column chromatography (100 g silica gel 60, 60% CHCl_3 /hexanes) followed by crystallization (EtOH) gave **2** (2.2 g, 61%) as a yellow powder: mp $62\text{--}64^\circ\text{C}$; ^1H NMR (CDCl_3) 3.39 (s, 3 H, CH_3), 3.56 (t, 2 H, CH_2OCH_3), 3.88 and 4.00 (t and t, 4 H, CH_2OCH_2), 4.32 (t, 2 H, CH_2OAr), 7.28–8.30 ppm (m, 7 H, Ar); IR (KBr) 1670, 1590, 1320, 1280, 1115, 985, 720 cm^{-1} . Anal. Calcd for $\text{C}_{19}\text{H}_{18}\text{O}_5$: C, 69.92; H, 5.57. Found: C, 69.81; H, 5.56.

1-(2-(2-(2-Methoxyethoxy)ethoxy)ethoxy)anthracene-9,10-dione (3). Triethylene glycol monomethyl ether (3.61 g, 22 mmol) was deprotonated as described above by using NaH (1.04 g, 26 mmol) in dry THF (15 mL), 1-chloroanthraquinone (2.7 g, 11.1 mmol) was rinsed in with dry THF (5 mL), and the mixture was stirred at ambient temperature for 20 h and then concentrated in vacuo. The residue was added to H_2O (100 mL) and extracted with CHCl_3 (130 mL). The organic phase was washed with brine (30 mL), dried (MgSO_4), and concentrated in vacuo. Column chromatography (90 g silica gel 60, 70% CHCl_3 /hexanes) followed by recrystallization (EtOH) gave **3** (2.5 g, 61%) as a yellow crystalline solid: mp $55\text{--}57^\circ\text{C}$; ^1H NMR (CDCl_3) 3.36 (s, 3 H, CH_3), 3.58–4.00 (m, 10 H, CH_2 's), 4.32 (t, 2 H, CH_2OAr), 7.26–8.25 ppm (m, 7 H, Ar); IR (KBr) 1670, 1590, 1320, 1270, 1100, 1070, 720 cm^{-1} . Anal. Calcd for $\text{C}_{21}\text{H}_{22}\text{O}_6$: C, 68.09; H, 6.00. Found: C, 68.08; H, 6.04.

1-(2-(2-(2-(2-Methoxyethoxy)ethoxy)ethoxy)ethoxy)anthracene-9,10-dione (4). Tetraethylene glycol monomethyl ether (2.3 g, 11 mmol) was deprotonated as described above by using NaH (0.63 g, 16 mmol) in dry THF (15 mL). The mixture was stirred for 45 min, and 1-chloroanthraquinone (2.7 g, 11.1 mmol) was rinsed in with dry THF (10 mL), then brought to reflux temperature, stirred for 6 h, cooled, and concentrated in vacuo. The residue was diluted with H_2O (50 mL) and extracted with CHCl_3 (2×50 mL). The combined organic phases were washed with brine (20 mL), dried (MgSO_4), and concentrated in vacuo. Column chromatography (100 g silica gel 60, 60% CHCl_3 /hexanes) followed by recrystallization (EtOH) gave **4** (3.0 g, 65%) as a yellow powder: mp $70\text{--}72^\circ\text{C}$; ^1H NMR (CDCl_3) 3.35 (s, 3 H, CH_3), 3.58–4.09 (m, 14 H, CH_2 's), 4.34 (t, 2 H, CH_2OAr), 7.30–8.26 ppm (m, 7 H, Ar); IR (KBr) 1670, 1590, 1320, 1270, 1155, 1140, 1120, 1100, 990, 720 cm^{-1} . Anal. Calcd for $\text{C}_{23}\text{H}_{26}\text{O}_7$: C, 66.64; H, 6.34. Found: C, 66.70; H, 6.38.

Preparation of 1-(2-Hydroxyethoxy)anthracene-9,10-dione. 1-Hydroxyanthraquinone (4.48 g, 0.02 mol), ethylene carbonate (3.52 g, 0.04 mol), tetrabutylammonium bromide (6.44 g, 0.02 mmol), and dry DMF (20 mL) were stirred at 170°C for 24 h under N_2 . The reaction was cooled and added to H_2O (150 mL). The precipitate was filtered, washed with cold H_2O (300 mL), and dried in vacuo (40°C , 0.1 mm). Column chromatography (120 g silica gel 60, CHCl_3) followed by recrystallization (THF) gave 1-(2-hydroxyethoxy)anthracene-9,10-dione (3.42 g, 64%) as a yellow powder: mp $164\text{--}166^\circ\text{C}$; ^1H NMR (CDCl_3) 3.65, 4.00 (br s and t, 3 H, CH_2OH), 4.30 (t, 2 H, CH_2OAr), 7.22–8.26 (m, 7 H, Ar).

1-(2-(*p*-Toluenesulfonyloxy)ethoxy)anthracene-9,10-dione. 1-(2-Hydroxyethoxy)anthracene-9,10-dione (see above, 2.0 g, 7.5 mmol) was dissolved in pyridine (2.0 mL), and CH_2Cl_2 (40 mL) was slowly added to a solution of *p*-toluenesulfonyl chloride (4.5 g, 23.5 mmol) in pyridine (4.5 mL) at 0°C . After addition, the reaction was warmed to ambient temperature and stirred for 48 h. The reaction was diluted with CH_2Cl_2 (60 mL) and washed consecutively with 6 N HCl (2×50 mL), H_2O (50 mL), and brine (50 mL). The organic phase was dried (MgSO_4) and concentrated in vacuo. Crystallization (*tert*-butanone) gave the title compound (2.3 g, 74%) as a yellow crystalline solid: mp $174\text{--}177^\circ\text{C}$; ^1H NMR (CDCl_3) 2.35 (s, 3 H, CH_3), 4.44 (s, 4 H, CH_2 's), 7.24–8.34 ppm (m, 11 H, Ar); IR (KBr) 1670, 1600, 1590, 1450, 1360, 1330, 1320, 1275, 1260, 1240, 1195, 1170, 940, 920, 820, 780, 720, 670 cm^{-1} . Anal. Calcd for $\text{C}_{23}\text{H}_{18}\text{O}_6\text{S}$: C, 65.38; H, 4.30. Found: C, 65.33; H, 4.30.

1-(2-(2-(2-(2-Methoxyethoxy)ethoxy)ethoxy)ethoxy)ethoxy)anthracene-9,10-dione (5). Tetraethylene glycol monomethyl ether (1.04

(11) For a general discussion of proton donor effects, see: *The Chemistry of the Quinonoid Compounds*; Patai, S., Ed. Wiley: New York, 1974; p 746.

(12) Stevenson, G. R.; Echegoyen, L.; Lizardi, L. *J. Phys. Chem.* **1972**, *76*, 143a.

(13) Fujita, M.; Furukawa, T.; Matsuo, M. *Chem. Pharm. Bull.* **1961**, *9*, 967.

g, 5.0 mmol) was added to a suspension of NaH (60% oil dispersion, 0.22 g, 5.5 mmol) in dry THF (10 mL) under N₂. After the mixture was stirred for 20 min, 1-(2-(*p*-toluenesulfonyloxy)ethoxy)anthracene-9,10-dione (1.06 g, 2.5 mmol) was added as a solid. The reaction mixture was brought to reflux temperature and stirred for 18 h. The mixture was cooled and concentrated in vacuo. The residue was added to H₂O (25 mL) and extracted with CHCl₃ (2 × 25 mL). The combined organic phases were washed with brine (10 mL), dried (MgSO₄), and concentrated in vacuo. Column chromatography (90 g silica gel 60, 60% CHCl₃/hexanes-2% MeOH/CHCl₃) followed by recrystallization (EtOH) gave **5** (160 mg, 14%) as a yellow powder: mp 48–49 °C; ¹H NMR (CDCl₃) 3.33 (s, 3 H, CH₃), 3.55–4.05 (m, 18 H, CH₂'s), 4.27 (t, 2 H, CH₂OAr), 7.22–8.22 (m, 7 H, Ar); IR (KBr) 1670, 1590, 1320, 1270, 1150, 1140, 1105, 990, 720 cm⁻¹. Anal. Calcd for C₂₅H₃₀O₈: C, 65.48; H, 6.61. Found: C, 66.64; H, 6.34.

1,8-Bis(1-oxaanthracene-9,10-dione)-3,6-dioxaoctane (6). Method A. Compound **6** was prepared from the potassium salt of 1-hydroxyanthraquinone (2.62 g, 0.01 mol), 1,2-bis(2-iodoethoxy)ethane (1.85 g, 0.005 mol), 18-crown-6 (2.64 g, 0.01 mol), and CH₃CN (30 mL) by a method analogous to that for the preparation of **7** (see procedure below). Column chromatography (silica gel 60, 2% MeOH/CHCl₃) followed by recrystallization (2-butanone) gave **6** (0.85 g, 30%) as a yellow powder: mp 173–175 °C; ¹H NMR (CDCl₃) 3.90, 4.03, and 4.30 (s, t, and t, 12 H, CH₂'s), 7.24–8.24 ppm (m, 14 H, Ar); IR (KBr) 1670, 1590, 1325, 1275, 715 cm⁻¹. Anal. Calcd for C₃₄H₂₆O₈: C, 72.58; H, 4.67. Found: C, 72.48; H, 4.71.

Method B. Triethylene glycol (3.75 g, 25 mmol) was slowly added to a vigorously stirred suspension of NaH (60% oil dispersion, 2.7 g, 68 mmol) in dry THF (40 mL) under N₂. After the mixture was stirred for 45 min, 1-chloroanthraquinone (12.13 g, 50 mmol) was added as a solid, and the flask was rinsed with dry THF (20 mL). The reaction mixture was brought to reflux temperature and vigorously stirred for 6 h. The mixture was cooled and concentrated in vacuo. The residue was added to H₂O (300 mL) and extracted with CHCl₃ (300 mL then 100 mL). The combined organic phases were washed with brine (100 mL), dried (MgSO₄), and concentrated in vacuo. Two recrystallizations (2-butanone) gave **6** (9.3 g, 66%) as a yellow powder (mp 146–148 °C solidifies and remelts at 175–177 °C). An analytically pure sample was obtained by passing 1 g of sample through a column of silica gel 60 (20 g, 2% MeOH/CHCl₃) followed by recrystallization (CH₃CN). Approximately 0.97 g of sample was recovered (mp 170–173 °C) which had physical properties identical with those reported above.

(Hydroxymethyl)-15-crown-5 was prepared as previously described¹⁴

(14) Dishong, D. M.; Diamond, C. J.; Cinoman, M. I.; Gokel, G. W. J. *Am. Chem. Soc.* 1983, 105, 586.

in 39% overall yield. The product had physical properties identical with those reported.

Preparation of 1-((1-Oxaanthracene-9,10-dione)methyl)-15-crown-5 (7). Method A. To a refluxing acetonitrile solution (20 mL) containing the potassium salt of 1-hydroxyanthraquinone (KHA, see above, 2.39 g, 9.1 mmol) and 18-crown-6 (2.41 g, 9.1 mmol) was added hydroxymethyl-15-crown-5 *p*-toluenesulfonate (2.5 g, 6.2 mmol) in acetonitrile (20 mL). After addition the reaction was heated at reflux for 3 days. After cooling, CHCl₃ (50 mL) and 3 N HCl (50 mL) were added. The phases were separated, and the aqueous portion was extracted with CHCl₃ (50 mL). The combined organic phases were washed with H₂O (25 mL) and brine (25 mL), dried (MgSO₄), and concentrated in vacuo. Column chromatography (silica gel 60, CHCl₃-5% MeOH/CHCl₃) gave an oil which crystallized on standing. The resulting solid was washed with EtOH to give **7** (1.1 g, 39%) as a yellow solid: mp 100–102 °C; ¹H NMR (CDCl₃) 3.68–4.22 (m, 21 H, aliphatic), 7.29–8.30 ppm (m, 7 H, Ar); IR (KBr) 1670, 1590, 1325, 1125, 715 cm⁻¹. Anal. Calcd for C₂₅H₂₈O₈: C, 65.77; H, 6.19. Found: C, 65.84; H, 6.24.

Method B. Hydroxymethyl-15-crown-5 (5.01 g, 20 mmol) in dry THF (15 mL) was slowly added to a vigorously stirred suspension of NaH (60% oil dispersion, 1.2 g, 30 mmol) in dry THF (15 mL) under N₂. After the mixture was stirred for 30 min, 1-chloroanthraquinone (4.85 g, 20 mmol) was added as a solid, and the flask was rinsed with dry THF (20 mL). The reaction was stirred at ambient temperature for 18 h and concentrated in vacuo. The residue was added to CHCl₃ (100 mL) and H₂O (50 mL). The phases were separated, and the aqueous portion was extracted with CHCl₃ (100 mL). The combined organic phases were washed with brine (50 mL), dried (MgSO₄), and concentrated in vacuo. Column chromatography (230 g, silica gel 60, 60% CHCl₃/hexanes-CHCl₃) followed by crystallization of the oily residue in EtOH gave **7** (3.6 g, 40%) with physical properties identical with those obtained by using method A.

Acknowledgment. We thank the National Institutes of Health for Grants (GM-31846, GM-33940, and GM-36262) and W. R. Grace & Co. which supported this work.

Registry No. 1, 82-39-3; 2, 104779-00-2; 3, 104779-01-3; 4, 104549-31-7; 5, 104779-02-4; 6, 104779-03-5; 7, 104084-69-7; HA, 129-43-1; KHA, 26035-17-6; Li⁺, 17341-24-1; Na⁺, 17341-25-2; K⁺, 24203-36-9; diethylene glycol monomethyl ether, 111-77-3; 1-chloroanthraquinone, 82-44-0; triethylene glycol monomethyl ether, 112-35-6; tetraethylene glycol monomethyl ether, 23783-42-8; 1-(2-hydroxyethoxy)anthracene-9,10-dione, 38933-94-7; 1-(2-(*p*-tolylsulfonyloxy)ethoxy)anthracene-9,10-dione, 104779-04-6; 1,2-bis(2-iodoethoxy)ethane, 36839-55-1; triethylene glycol (hydroxymethyl)-15-crown-5-*p*-toluenesulfonate, 84131-00-0; (hydroxymethyl)-15-crown-5, 75507-25-4; ethylene carbonate, 96-49-1.

Unusually Facile Dissociation of Benzene by Ruthenium Metal

J. A. Polta and P. A. Thiel*

Contribution from the Department of Chemistry and Ames Laboratory, Iowa State University, Ames, Iowa 50011. Received July 16, 1986

Abstract: Associative chemisorption of benzene at room temperature has been reported on several group VIII metal surfaces (Ni, Rh, Pd, Pt), where molecular adsorption is followed by partial dissociation and partial desorption at higher temperatures. However, we find that between one-fourth and one-half of a full layer of benzene adsorbs *irreversibly* at 85 K into a state which represents either a dissociated form of benzene or a molecular precursor to dissociation. Those molecules which subsequently adsorb do not dissociate and can desorb in several states between 120 and 180 K. For these, the chemisorption bond is very weak, only 9–11 kcal/mol. We propose that this is true because the Ru surface is electronically or sterically modified by the dissociative phase. Coadsorbed water can prevent decomposition but cannot displace benzene from the dissociative phase. Furthermore, the adsorbed benzene surface layer acts as a template for growth of a metastable benzene multilayer, which has a heat of sublimation of 7 ± 1.4 kcal/mol. The metastable multilayer is eventually converted completely to normal bulk benzene at very high coverages. The data are obtained from several types of experiments: multiple-mass thermal desorption spectroscopy of benzene itself, quantitative oxidation of residual carbon, and competitive coadsorption of benzene and water.

(I) Introduction

There is a large body of literature which describes the chemisorption of benzene on low-index, single-crystal surfaces of Ni, Rh, Pd, and Pt.¹⁻¹⁷ These studies have generally dealt with a

saturated chemisorbed layer at room temperature, and certain conclusions are common to all of them: (1) Benzene adsorbs

(1) Demuth, J. E.; Eastman, D. E. *Phys. Rev. Lett.* 1974, 32, 1123.